

FREQUENCY MAPS OF LHC MODELS

Y. Papaphilippou*

CERN, CH-1211 Geneva 23, Switzerland

Abstract

The Frequency Map Analysis method is applied in models of LHC optics versions 5 and 6 in order to study their non-linear dynamics. The maps present a global picture of the resonance structure of the phase space. They enable us to view the dangerous zones tracing the limits of the dynamic aperture. This approach, assisted by detailed resonance analysis, is used as a guide for exploring possible correction schemes, which are subsequently verified by long-term tracking.

1 INTRODUCTION

The long term stability of the beam is the major concern for the design of a hadron collider, as the LHC [1]. Especially during long injection period of more than 10^7 turns needed to fill the LHC with 2835 bunches per beam, particle trajectories are perturbed strongly by non-linear magnet fields, mainly attributed to the multipole errors of the superconducting magnets. In order to estimate the dynamic aperture (D.A.), the region of the phase space where particles survive after a long time, particle tracking is usually employed, with codes optimised for this task [2, 3]. Nevertheless, even in the upgraded multiprocessor system now available at CERN [4], tracking studies of the full injection plateau are extremely time consuming. Simulations are thus limited to 1% of the total injection period and a reduction factor of 7% [5, 6] is taken into account for the estimation of the D.A. [7]. Beside the numerical difficulties, the main drawback comes from the fact that tracking cannot provide enough information about the system's phase space structure. The application of high-order perturbation theory has been extensively used in beam physics [8, 9] in order to give some insight regarding the systems' non-linear dynamics. However, the construction of some optimal set of variables (normal forms or action-angle) for the evaluation of the phase space distortion cannot be applied in the parts of the phase space which are close to instabilities, such as resonances or chaotic regions. In fact, an approach giving in a direct way a global view of the phase space structure is needed. This later can be achieved by the Frequency Map Analysis (F.M.A), a method extensively used in celestial mechanics [10, 11] and in Hamiltonian toy models [12–14] but only recently in real accelerators, as the ALS [15] or the LHC [7]. The method relies on the high precision calculation [18] of another fixed feature of KAM orbits, the associated frequencies of motion and can be directly applied in short term tracking data. Moreover, the variation of the frequencies over time [7, 13, 14] can provide an early stability indicator as good as, if not better

than, the Lyapounov exponent.

After a brief introduction to the method (Sect. 2), we display in frequency maps the global dynamics for cases of interest of LHC optics version 5 and 6, show many interesting features of the phase space structure and demonstrate the efficiency of the method in comparing different designs through a diffusion quality factor (Sect. 3). The last section is devoted to the final conclusions and perspectives.

2 FREQUENCY MAPS

The first step is to derive through the NAFF algorithm [10] or variants of this code (e.g. SUSSIX [17]), a quasi-periodic approximation, truncated to order N ,

$$f'_j(t) = \sum_{k=1}^N a_{j,k} e^{i\omega_{jk}t}, \quad (1)$$

with $f'_j(t)$, $a_{j,k} \in \mathbb{C}$ and $j = 1, \dots, n$, of a complex function $f_j(t) = q_j(t) + ip_j(t)$, formed by a pair of conjugate variables of a n degrees of freedom Hamiltonian system, which are determined by usual numerical integration, for a finite time span $t = \tau$. The next step is to retain from the quasi-periodic approximation the frequency vector $\nu = (\nu_1, \nu_2, \dots, \nu_n)$ which, up to numerical accuracy [18], parameterises the KAM tori in the stable regions of a non-degenerate Hamiltonian system. Then, the construction of the frequency map can take place [12–15], by repeating the procedure for a set of initial conditions which are transversal to the orbits of interest. As an example, we may keep all the q variables constant, and explore the momenta p to produce the map \mathcal{F}_τ :

$$\mathcal{F}_\tau : \begin{array}{l} \mathbb{R}^n \longrightarrow \mathbb{R}^n \\ p|_{q=q_0} \longrightarrow \nu \end{array} \quad (2)$$

The dynamics of the system is then analysed by studying the regularity of this map.

3 APPLICATION TO THE LHC

The F.M.A is applied to the short-term tracking data ($\tau = 10^3$ turns) issued by SIXTRACK [3], for a large number of initial conditions ($\approx 10^4$). We select an arbitrary section of the phase space, setting the initial transverse momenta to zero. The particle coordinates are chosen equally spaced in the transverse linear Courant-Snyder invariants I_{x0} and I_{y0} , at different ratios I_{x0}/I_{y0} . Hence, we construct the map

$$\mathcal{F}_\tau : \begin{array}{l} \mathbb{R}^2 \longrightarrow \mathbb{R}^2 \\ (I_x, I_y)|_{p_x, p_y=0} \longrightarrow (\nu_x, \nu_y) \end{array}, \quad (3)$$

and proceed to the dynamical analysis of the accelerator model.

* Email: yannis@mail.cern.ch

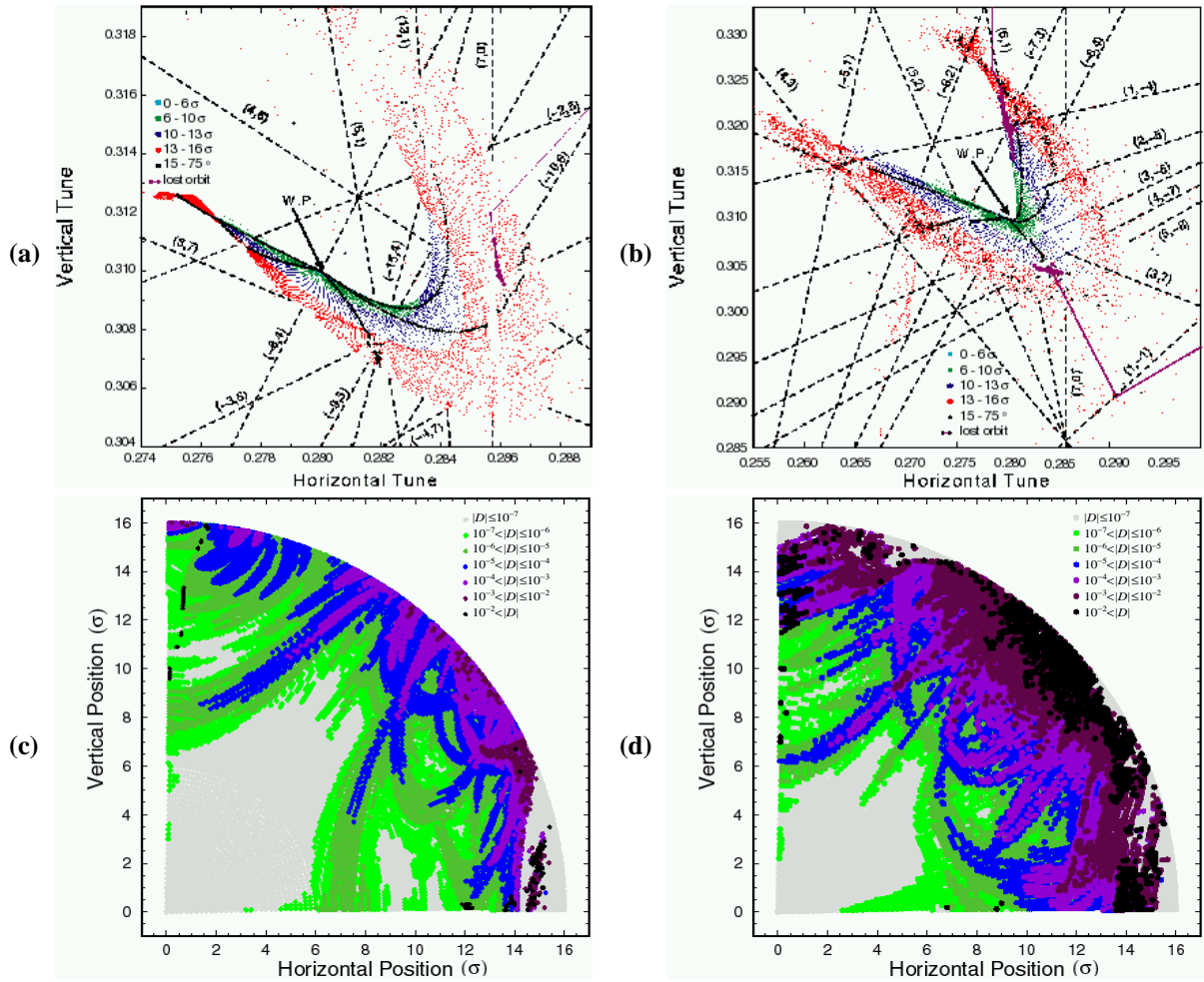


Figure 1: Frequency and amplitude maps for LHC optics version 5 target table without ((a),(c)) and with ((b),(d)) the high a_4 value of error table 9712 on the dipoles.

In order to reach the target D.A. of 12σ for the LHC injection optics, giving a necessary safety factor of 2 with respect to the position of the collimators at 6σ , a target error table was proposed. A frequency map for optics version 5 with this error table and for the nominal working point ($Q_x = 63.28$, $Q_y = 59.31$) is shown in Fig. 1a. This specific machine gives an average D.A. over 11 different invariant ratios of 13.1σ and a minimum of 12.1σ (at $\arctan(I_{y0}/I_{x0}) = 15^\circ$), values which are close to the average and minimum D.A. over all the 60 random realisation of the magnet errors (“seeds”) usually produced for 6D tracking. Each point in the frequency space corresponds to a different orbit. The different colours in the map correspond to orbits with different initial amplitude $I = \sqrt{I_x^2 + I_y^2}$ (from $0 - 16\sigma$) and the black dots label initial conditions with different ratios (from 15° to 75°). The orderly spaced points correspond to regular orbits whereas the dispersed points to chaotic ones. This plot is a snapshot of the so called Arnold web, the complicated network of resonances $a\nu_x + b\nu_y + c = 0$, which appear as distortion of the map (empty and filled lines) and can be easily identified. For example, we put in evidence the importance of three 7th order resonances $((a, b) = (7, 0), (6, -1)$ and $(-2, 5)$). Especially, the crossings of the

resonant lines are “hot spots”, from which particles can easily diffuse: as an example, we show the evolution of the frequency of an orbit starting close to the crossing of the $(7, 0)$ with the $(-3, 6)$ and $(4, 6)$ resonances. The orbit diffuses along the unstable manifold of the 7th order resonance and is lost after a few thousand turns. This is a clear demonstration of the importance of this resonance with respect to the D.A. of this model.

One of the main issues in the specification of the LHC injection optics, is the correction of the systematic part of the lowest order multipole errors of the super-conducting dipoles, which limit the D.A. [6]. This is usually done by magnetic coils (“spool pieces”) placed at the ends of the dipoles. In the case of the last 9712 error table, where biases of the normal and skew octupoles have been significantly raised, there was an important loss of the dynamic aperture [19] with respect to the target error table. A frequency map for the same “seed” as for the previous case with the skew octupole error of the 9712 table in the dipoles is shown in Fig. 1b. The phase space now looks much more distorted. The most remarkable feature concerning the system’s dynamics is the explosion of the detuning, to the point that particles, especially the ones with initial amplitude ratio of 45° are diffusing towards the diagonal

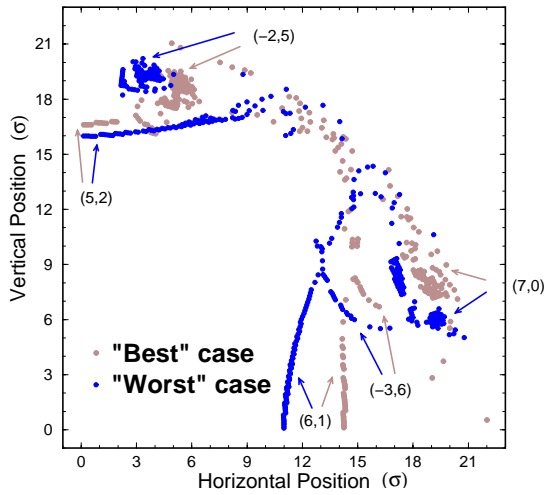


Figure 2: Positioning of the main resonances the initial amplitude space for two different correction schemes of the b_4 , b_5 error on the main dipoles of LHC optics version 6.

$(1, -1)$ in the right corner of the map. On the other hand, particles close to horizontal motion at the top of the map are approaching the $(0, 3)$ resonance and the ones close to vertical motion the $(4, 0)$. This finding has been confirmed with Normal Form analysis. The dynamic aperture could be recovered by tuning the skew octupole spool pieces such as to cancel the $(1, -1)$ resonance [19]. The global dynamics of these two cases can be also displayed in the physical space of the system by mapping each initial condition with a diffusion indicator: the tune can be calculated for two equal and successive time spans which correspond to half of the total integration time τ , giving a diffusion vector:

$$D|_{t=\tau} = \nu|_{t \in (0, \tau/2]} - \nu|_{t \in (\tau/2, \tau]}, \quad (4)$$

the amplitude of which can be used for characterising the instability of each orbit. In Figs. 1c and d, we plot the points in the (I_{x0}, I_{y0}) -space with a different colour corresponding to different diffusion indicators in logarithmic scale: from grey for stable ($|D| \leq 10^{-7}$) to black for strongly chaotic particles ($|D| > 10^{-2}$). Through this representation we are able to view the traces of the resonances in the physical space, and set a pessimistic threshold for the minimum D.A.. Moreover, we can compute a diffusion quality factor defined as the average of the local diffusion coefficient to the initial amplitude of each orbit, over a domain R of the phase space:

$$D_{QF} = \left\langle \frac{|D|}{(I_{x0}^2 + I_{y0}^2)^{1/2}} \right\rangle_R. \quad (5)$$

This quantity can be used for the comparison of different designs and the optimisation of the correction schemes proposed. For example, for the normal octupole and decapole correction of LHC optics version 6, five schemes were proposed, regarding the positioning of the “spool pieces”. In Fig. 2, we display the strongly excited resonances (four of 7th and one 9th order) in the amplitude space for the best and worst case, as suggested by the diffusion quality factor. The best one corresponds to the nominal scheme, where the

“spool pieces” are positioned in every dipole and correct the average value of b_4 and b_5 systematic per arc, whereas the worst machine corresponds to a correction with spool pieces in every second dipole. In both cases only the systematic per arc b_4 and b_5 errors are switched on, which explains the relatively weak distortion of the phase space for small amplitudes. On the other hand, in the “bad” case, the dangerous resonances are shifted towards lower amplitudes, as the detuning is higher, especially for horizontal motion. In fact, this correction option is not good for the LHC, due to the odd number of dipoles per half cell.

4 CONCLUSIONS

The F.M.A. was employed for the thorough study of the dynamics of different LHC machines with the injection optics version 5 and 6. All the fine details of the systems’ phase space are directly viewed in frequency maps. Through the evolution of the tunes with time, the drifting of chaotic orbits is followed in the frequency space and different types of diffusion are shown. Moreover, the tune difference for two successive time spans enables the representation of the resonance structure and phase space distortion on the initial amplitude space. This instantaneous diffusion coefficient allows the computation of a global quality factor which can be efficiently used for comparison of different accelerator models with respect to their phase space stability. The method can be applied to the study of many open problems regarding the LHC non-linear dynamics, as the beam-beam effect, the optimal choice of the working point and its sensitivity to small variations or the influence of tune modulation. For this, it is envisaged to extend the approach to the full 6D phase space. Indeed, the challenge will be to establish the statistical correlation of early indicators such as the frequency variation with the beam lifetime.

5 REFERENCES

- [1] The LHC Study Group, CERN/AC/95-05(LHC), (1995).
- [2] H. Grote and F.C. Iselin, CERN-SL-90-13-AP, (1990).
- [3] F. Schmidt, CERN-SL-94-56-AP, (1994).
- [4] E. McIntosh, et al., LHC95 Workshop, Montreux, (1995).
- [5] M. Böge and F. Schmidt, PAC’97, Vancouver, (1997).
- [6] J.P. Koutchouk, this conference.
- [7] M. Giovannozzi, et al., Part. Accel. 56, 195, (1997).
- [8] M. Berz, et al., Part. Accel. 24, 91 (1989).
- [9] A. Bazzani, et al., CERN Yellow Report, 94-02, (1994).
- [10] J. Laskar, Astron. Astroph. 198, 341, (1988).
- [11] J. Laskar, Icarus 88, 266, (1990).
- [12] J. Laskar, et al., Physica D 56, 253, (1992).
- [13] J. Laskar, Physica D 67, 257 (1993).
- [14] H.S. Dumas and J. Laskar, Phys. Rev. Let. 70, 2975, (1993).
- [15] J. Laskar and D. Robin, Part. Acc. 54, 183, (1996).
- [16] E. Todesco, et al., EPAC’96, Barcelona, (1996).
- [17] R. Bartolini and F. Schmidt, CERN-SL-98-17-AP, (1998).
- [18] J. Laskar, NATO-ASI, S’Agaro, Spain, unpublished.
- [19] Y. Papaphilippou, et al., LHC Project Report 253, (1998).